

A FULL FIELD-MAP MODELING OF CORNELL-BNL CBETA 4-PASS ENERGY RECOVERY LINAC*

F. Méot[†], N. Tsoupas, S. Brooks, D. Trbojevic, BNL C-AD, Upton, NY, USA
J. Crittenden, Cornell University (CLASSE), Ithaca, NY, USA

Abstract

The Cornell-BNL Electron Test Accelerator (CBETA), a four-pass, 150 MeV energy recovery linac (ERL), is now in construction at Cornell. Commissioning will commence in March 2019. A particularity of CBETA is that a single channel loop recirculates the four energies (42, 78, 114 and 150 MeV). The return loop arcs are based on fixed-field alternating gradient (FFAG) optics. The loop is comprised of 107 quadrupole-doublet cells, built using Halbach permanent magnet technology. Spreader and combiner sections (4 independent beam lines each) connect the 36 MeV linac to the FFAG arcs. We introduce here to a start-to-end simulation of the 4-pass ERL, entirely, and exclusively, based on the use of magnetic field maps to model the magnets.

INTRODUCTION

The Cornell-BNL Electron Test Accelerator (CBETA), a four-pass, 150 MeV energy recovery linac (ERL), is now in construction at Cornell. A particularity of CBETA is in its single channel loop recirculating four energies, 42, 78, 114 and 150 MeV, four-pass up, four-pass down. The return loop arcs (FA-TA and TB-FB sections, Fig. 1) are based on fixed-field alternating gradient (FFAG) optics. The loop is comprised of 107 quadrupole-doublet cells, built using Halbach permanent magnet technology. Spreader (SX) and combiner (RX) sections (4 independent beam lines each) connect the 36 MeV linac to the FFAG arcs. This paper introduces to a start-to-end simulation of the 4-pass ERL, entirely, and exclusively, based on the use of magnetic field maps to model the magnets, now under development in view of the commissioning of CBETA which will commence in March 2019.

The OPERA field maps of the return loop Halbach magnets are produced at BNL. The OPERA field maps of most of the spreader and combiner line conventional electro-magnets are produced at Cornell.

Why Use Field Maps?

There is a variety of reasons for that:

- All necessary material is available or will soon be: the return loop Halbach magnet field maps have been produced during the design [1], the spreader and combiner section conventional magnet field maps (dipoles and quadrupoles) are under production. Thus, as it yields highest simulation accuracy, why not just do it? And,

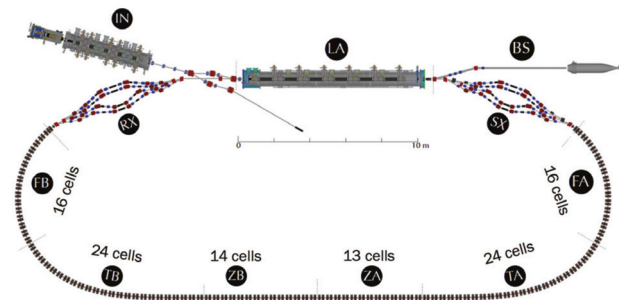


Figure 1: CBETA 150 MeV ERL [2]. The linac is 36 MeV, four different energies circulate concurrently in the single-channel return loop: 42, 78, 114 and 150 MeV (hence, 4 spreader (SX) and recombiner lines (RX), at linac downstream and upstream ends, respectively).

in passing, forget about questionable mapping approximations.

- FFAG experience dictates to do so: as early as in the 1950s, Frank Cole wrote on the virtues of the use of field maps and Runge-Kutta ray-tracing in designing and operating the MURA scaling FFAG rings [3]:

"[...] digital computation to explore nonlinear problems in spiral-sector orbits. This was not done by mapping in the usual sense of the term, but by step-by step integration of the equations of motion, using the fourth-order Runge-Kutta method. It was a marvelous productive year for the [MURA] group."

Kyushu University and KURRI 150 MeV scaling FFAG proton rings (amongst others in Japan) were designed, and are operated, using 3D OPERA field maps of the cell dipoles [4]; the RACCAM spiral FFAG dipole constructed and measured in 2009 was designed and optimized, successfully, based on field map simulations [5–7]; the optics of the EMMA linear FFAG ring accelerator at Daresbury (CBETA arc cell is similar to EMMA's) was studied using OPERA field maps of its QF-QD cell magnets [8].

- Using field maps yields closest-to-real-life modeling of the Halbach doublets return loop, over the all 8 passes (4 accelerated, 4 decelerated).

Now, the method must be validated. This will be discussed here and includes showing the feasibility of

- using separate field maps, especially of the QF and BD focusing quadrupole and combined function defocusing dipole in the return loop,
- including field overlapping between neighboring magnets, all along the return loop,
- and accounting for iron yoke corrector magnets superimposed on the Halbach magnets.

* Work supported by Brookhaven Science Associates, LLC under Contract No. DE-AC02-98CH10886 with the U.S. Department of Energy

[†] fmeot@bnl.gov

Content from this work may be used under the terms of the CC BY 3.0 licence (© 2018). Any distribution of this work must maintain attribution to the author(s), title of the work, publisher, and DOI.

The interest of using separate field maps is in the flexibility in the modeling, allowing in particular,

- independent fine-tuning of QF, QD and BD Halbach magnet strengths,
- an independent power-supply knob for each corrector field map,
- the possibility of independent field and positioning errors and compensation,
- easier connection between CBETA sectors (FA, TA, ZA, etc., Fig. 1).

OVERVIEW

The rest of this technical note consists in a series of figures with self-explanatory captions (Figs. 2–14), together with some comments and sample input data lists to the ray-tracing code used in this modeling of CBETA [9, 10]. This Section gives an overview of the methods and present outcomes. This is a work in progress, thus this note will conclude on partial completion, the plan being to have a complete simulation in due time, in particular a 1-pass up, 1-pass down loop ready for the start of the commissioning.

Note that the code used is under development at Radiasoftware [11], which includes its installation in the SIREPO environment [12]. Figure 2 shows preliminary aspects of the latter, more is to come in near future.

OPERA Simulation of CBETA Arc Cell

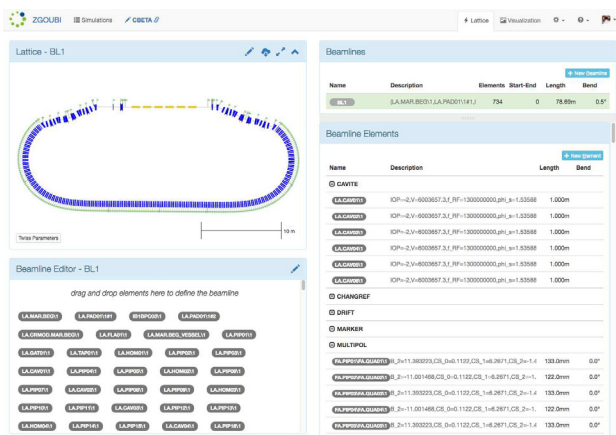


Figure 2: Layout of the CBETA 42 MeV pass, in SIREPO environment [12].

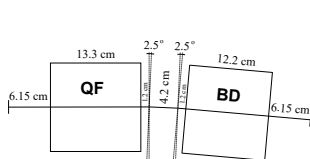


Figure 3: CBETA FFAQ QF-BD cell in the FA and FB sections of the arcs (Figs. 1, 4). Figure 4: SX and FA-TA arc.

Optical sequence of the arc cell (Fig. 3) in Zgoubi, case of a single full-cell field map:

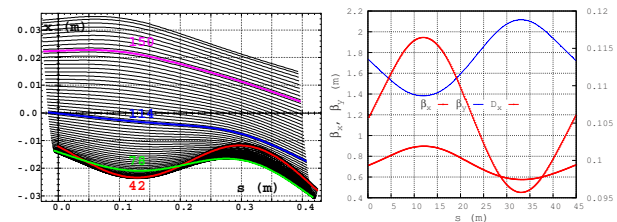


Figure 5: An energy scan of the orbits across the arc cell, including the 4 design energies (left) and the 42 MeV optical functions (right), derived from the OPERA field maps modeling of the QF and BD Halbach magnets.

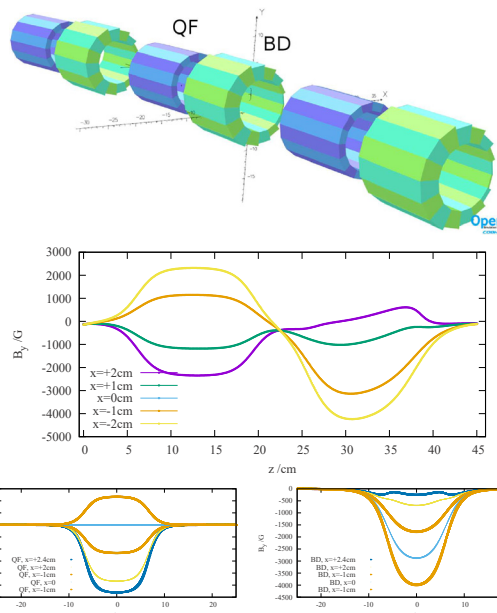


Figure 6: Top: the OPERA field map of a full cell is computed from the middle QF-BD doublet of a series of three, to ensure periodicity of the field. Middle: the resulting mid-plane field across the cell, samples taken at various distances x from the cylinder axis. Bottom: mid-plane field across the magnets, at various distances x from the cylinder axis, case of separate computation of the two field maps.

```
'TOSCA' QF+BD
0 0
-9.69871600E-04 1.000 1.000 1.000
HEADER_8 ZroBXY
451 83 27 15.1 1.
3cellFieldMap.table
1 -508.5 44.49 2.2E4 ! MOTION BOUNDARY
2
.2
2 0.000 0.000 0.000
'CHANGREF'
XS -0.678391 YS -1.8870962 ZR -5.0
```

Optical sequence of the arc cell (Fig. 3) in Zgoubi, case of separate QF, BD maps:

```
'DRIFT'
6.15
'DRIFT'
-18.35 !=(50cm - 13.3cm)/2 (50cm is field map extent)
'TOSCA' QF
0 0
-9.76E-04 1. 1. 1.
HEADER_8 ZroBXY
501 83 1 15.1 1.
```

Content from this work may be used under the terms of the CC BY 3.0 licence (© 2018). Any distribution of this work must maintain attribution to the author(s), title of the work, publisher, and DOI.

```

QF-3D-fieldMap.table
0 0 0
2
.2
2 0.00E+00 0.00E+00 0.00E+00
'DRIFT'
-18.35 ! =(50cm - 13.3cm)/2 (50cm is field map extent)
'DRIFT' ED1
1.2
'CHANGREF' CORNER
ZR -2.50
'DRIFT' BPM
4.2
'CHANGREF' CORNER
ZR -2.50
'DRIFT' ED1
1.2
'DRIFT'
-18.9 ! =(50cm - 12.2cm)/2 (50cm is field map extent)
'TOSCA' BD
0 0
-9.76E-04 1.00E+00 1.00E+00 1.00E+00
HEADER_8 ZroBXY
501 83 1 15.1 1.0
BD-3D-fieldMap.table
0 0 0
2
.2
2 0. -.019 0. ! Y-offset -0.019cm = inward
'DRIFT'
-18.9 ! =(50cm - 12.2cm)/2 (50cm is field map extent)
'DRIFT' HD2
6.15
    
```

Beam Optics Validations

1: First order parameters of the arc cell They are displayed in Figs. 7 and 8. Table 1 details the path length at the four design energies, depending on the field map modeling method. Differences do not exceed a few ppm.

Table 1: Path Length, Detailed Values

Path length across cell (cm)				
E (MeV)	42	78	114	150
Single 3D map	44.4846	44.3298	44.3898	44.5806
Two 2D or 3D maps	44.4845	44.3291	44.3884	44.5797

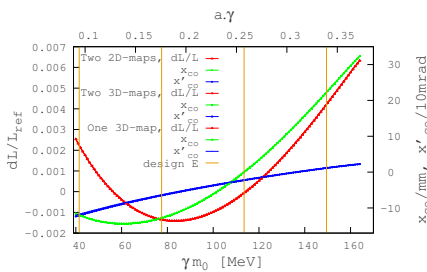


Figure 7: Separate 2D or 3D field maps of QF and BD, or 3-D full-cell single map, yield the same closed orbit coordinates (at the center of the long drift, here), and the same trajectory lengthening, all superimposed on this graph.

2: Dynamical admittance The dynamical admittance at a given energy, here, is taken as the maximum stable invariant that makes it through a 400 cell channel, for that energy: beyond that invariant, particles get kicked away under the effect of field or kinematical non-linearities. Results are displayed in Fig. 9.

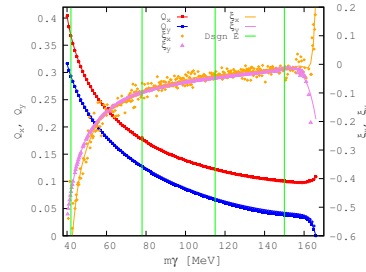


Figure 8: Separate 2D or 3D field maps of QF and BD, or 3-D full-cell single map, yield same paraxial tunes and chromaticities.

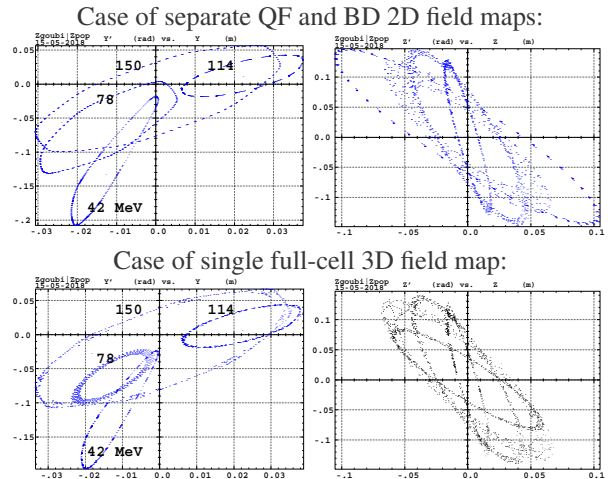


Figure 9: Left column: horizontal motion; right column: vertical motion. Observation plan is at the middle of the long drift. Non-linearities at the origin of the limited amplitude are from the field and from kinematic terms in the motion. The maximum invariant values are ~meter normalized, they are comparable in the two cases, two separate field maps of a single full-cell map - and far beyond μm CBETA beam emittance.

3: Dynamical admittance, energy scan A similar exercise to the previous one, repeated for a series of energies ranging from 39 to 170 MeV (Fig. 10).

Closer to CBETA FFAG Cell

We want the cell model even fancier, Fig. 11. Namely, including the H and V orbit correction dipoles (iron yoke electromagnets), on top of respectively the F and D Halbach FFAG magnets. This requires two independent field maps. In the case of a full-cell single field map for instance, as was done for the EMMA FFAG ring [8], each one of the two additional field maps comprises the corrector pair, however,

- one corrector pair field map has the F-corrector on and the D-corrector off,
- the other one has the F-corrector off and the D-corrector on. This allows independent knobs for these correctors.

The complete return loop is at present operational, fully field-map.

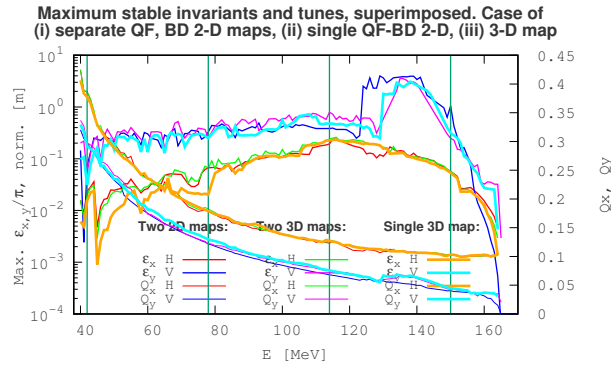


Figure 10: “H”: horizontal motion (initial V invariant is taken very small). “V”: vertical motion (initial H invariant is taken very small). The DA curves in this graph are the surfaces of the phase space curves as shown in Fig. 9, repeated for different energies. The H and V tunes are for these maximum invariants, computed using a DFT. It can be seen that the 42 MeV beam is placed away from the Walkinshaw resonance (the dip in the vertical acceptance, to the left of the 42 MeV vertical bar), and from the $Q_x = 1/3$ resonance (the dip in the horizontal acceptance, to its right). The superimposition shows that the three different field map models yield comparable results.

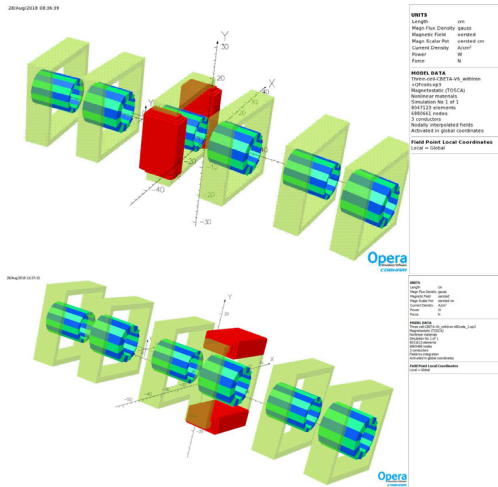


Figure 11: OPERA simulation of the full-cell H and V orbit correction dipoles (iron yoke electromagnets), on top of respectively the F and D Halbach FFAG magnet.

Code sequence for an arc cell, case of single full-cell field maps:

```
'TOSCA' QF+BD map + corrector maps
0 0
-9.69871600E-04 1. 1. 1.
HEADER_8 ZroBXY
451 83 27 15.3 1. 0.001 0.001 ! 3 independent knobs
3D-Cell-fieldMap.table ! FFAG qf-BD doublet
FConDCoff-3D-fieldMap.table ! F corrector
FCoffDCon-3D-fieldMap.table ! D corrector
1 482.028 42.172 -20328 ! integration boundary
2
.2 ! integration step size
2 0.0 0.0 0.0 ! magnet positioning
'CHANGREF' ! magnet positioning:
XS -0.6586 YS -3.2061 ZR -5.0 YS 1.2047
```

Code sequence for an arc cell, case of separate QF, BD and corrector field maps:

```
'DRIFT'
5.6 -18.35
'TOSCA' QF
0 0
-9.69871600E-04 1.00E+00 1.00E+00 1.00E+00
HEADER_8 ZroBXY
501 83 1 15.2 1. 0.
QF-2D-fieldMap.table
FCorr-2D-fieldMap.table
0 0 0 0
2
.1
2 0.00E+00 0.00E+00 0.00E+00
'DRIFT'
-18.35
'DRIFT'
1.2
'CHANGREF' CORNER
ZR -2.50
'DRIFT'
4.2
'CHANGREF' CORNER
ZR -2.50
'DRIFT'
1.2
'DRIFT'
-18.9
'TOSCA'
0 0
-9.69871600E-04 1.00E+00 1.00E+00 1.00E+00
HEADER_8 ZroBXY
501 83 1 15.1 1.0
501 83 1 15.2 1. 0.
BD-2D-fieldMap.table
DCorr-2D-fieldMap.table
0 0 0 0
2
.1
2 0.00E+00 3.60319403E-04 0.00E+00
'DRIFT'
-18.9 + 6.7
```

SX and RX line models in Zgoubi are under construction, replacing the analytical field model of the dipole and quadrupoles by their field map, step by step. Any such change of an optical element causes a slight change in the optical functions, Fig. 12, necessitating a retuning of the orbit and optical functions (textsli.e., re-matching between SX (or RX) and the FFAG arc).

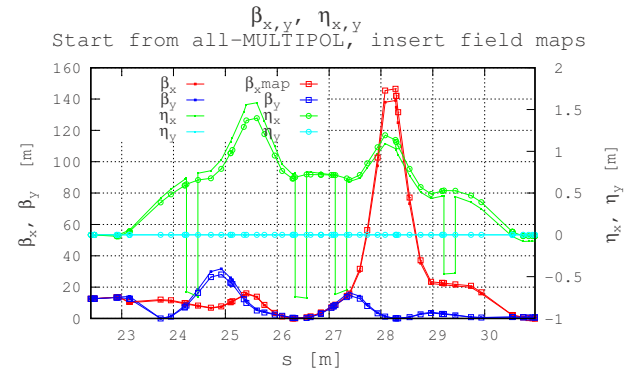


Figure 12: A change in the modeling of an element along the line (SX here, 42 MeV spreader line), from an analytical field model to its OPERA field map, perturbs the optics and necessitates a re-matching of the orbit and optical functions.

REFERENCES

- [1] F. Méot *et al.*, “Beam dynamics validation of the Halbach Technology FFAg Cell for Cornell-BNL Energy Recovery Linac”, *NIM A*, vol. 896, pp. 60-67, 2018.
- [2] J. Barley *et al.*, *CBETA Design Report*, Jan 2017.
- [3] F. T. Cole, “O Camelot ! A Memoir of the MURA Years,” April 1, 1994, <http://jacow.org/c01/cyc2001/extra/Cole.pdf>
- [4] See the FFAg workshop series: <https://www.bnl.gov/ffag17/pastWorkshops.php>
- [5] F. Méot, “RACCAM: A status, including magnet prototyping and magnetic measurements”, FFAg 2009 Workshop, Fermilab, Batavia, IL, USA. <https://indico.fnal.gov/event/2672/session/2/contribution/8/material/slides/1.pdf>
- [6] S. Antoine *et al.*, “Principle design of a protontherapy, rapid-cycling, variable energy spiral FFAg,” *NIM A*, vol. 602, pp. 293–305, 2009.
- [7] T. Planche *et al.*, “Design of a prototype gap shaping spiral dipole for a variable energy protontherapy FFAg,” *NIM A*, vol. 604, pp. 435-442, 2009.
- [8] Y. Giboudot and F. Méot, “Optical matching of EMMA cell parameters using field map sets,” in *Proc. PAC’09*, Vancouver, BC, Canada, paper TH5PFP040.
- [9] https://zgoubi.sourceforge.io/ZGOUBI_DOCS/Zgoubi.pdf
- [10] <https://www.osti.gov/scitech/biblio/1062013-zgoubi-users-guide>
- [11] D. Abell, “Zgoubi: Recent Developments and Future Plans”, presented at ICAP2018, Key West, FL, USA, paper TUPAF04, this conference.
- [12] P. Moeller, Radiasoft, priv. comm., Oct. 2018. “An interface to accelerator codes” <https://beta.SIREPO.com/#/accel>

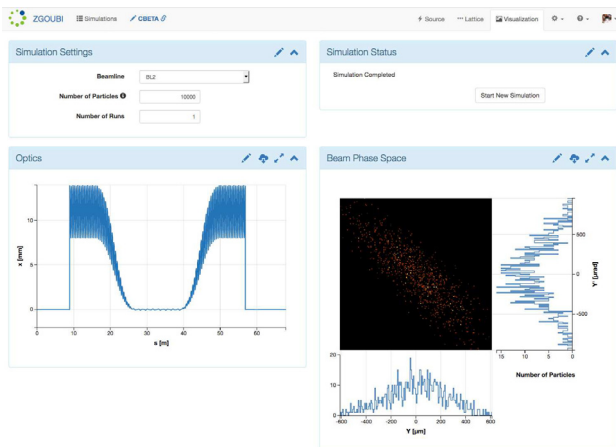


Figure 13: Working on the first turn (42 MeV) in SIREPO environment [12]. The orbit around the loop is shown, here, together with the projection of a bunch in the horizontal phase-space after a turn from linac exit to linac entrance.

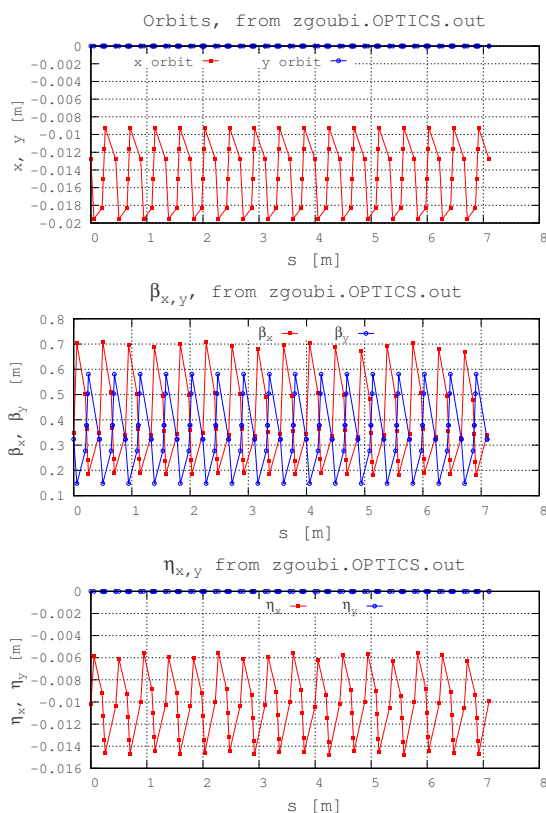


Figure 14: 42 MeV orbit and optical functions in TA arc, observed at a few points along the cell (lines are to guide the eye).

Content from this work may be used under the terms of the CC BY 3.0 licence (© 2018). Any distribution of this work must maintain attribution to the author(s), title of the work, publisher, and DOI.